

# COHERENT STRUCTURES OF SUSPENSION FLOW AND THEIR INHERITANCE IN PAPER

*Petri Jetsu<sup>1</sup>, Markku Kellomäki<sup>2</sup>, Hannu Karema<sup>2</sup>,  
Juha Salmela<sup>2</sup>, Timo Lappalainen<sup>2</sup> and Mika Piirto<sup>3</sup>*

<sup>1</sup>Metso Paper Inc., P.O. Box 587, FIN-40101 Jyväskylä, Finland

<sup>2</sup>VTT Energy, Technical Research Centre of Finland,

P.O. Box 1603, FIN-40101 Jyväskylä, Finland

<sup>3</sup>Tampere University of Technology, Energy and Process Engineering,  
P.O. Box 589, FIN-33101 Tampere, Finland

## ABSTRACT

Normally, the main purpose of vanes installed in the slice chamber of a hydraulic headbox is to control the tensile strength ratio by affecting the mean fiber orientation of the suspension. The use of vanes inherently leads to the formation of peculiar vortex structures, referred to here as coherent flow structures (CS), in the downstream flow. These CS are believed to produce non-homogeneity in paper. Although the CS are geometrically three dimensional, their machine direction (MD) and cross direction (CD) components are dominant, cf. Kármán vortex street, and have distinctive characters of their own. The CD component of the vortex maintains its coherent nature better than the MD component and, therefore, its appearance in a form of MD spatial scale is used to express the inheritance of the flow structures in the paper. By using bluff vanes of different thicknesses, it is shown that the CD component of the vortex street maintains its characteristic appearance from the slice chamber to the slice jet. This made it possible to study the inheritance of flow structures in paper with more realistic vanes. By marking particular parts of

the flow in the slice chamber with dye streamers the CS were also made visible in the paper. An analysis of these samples reveals that the average scale of ink spots is related to the MD spatial scale of flow structures. Finally, a correlation between the CS of flow and the structural cockling tendency was found. Thus, important complementary information has been created to serve the goal of finding a general linkage between structures in flow and paper. The knowledge of this link would not only allow research and analysis of wet end operations without actually producing paper, but would also provide a means of evaluating wet end conditions in a mill environment by paper analysis.

## 1 INTRODUCTION

In a slice chamber, several mechanisms leading to coherent flow structures in particular flow conditions or classes of flow exist. In turbulent internal flows the boundary layer itself contains strong coherent structures (CS) both in the stream-wise (MD) and the span-wise (CD) directions [1]. In fact, the sequence of events leading to production of turbulence, a vital phenomenon for turbulent flows in general, includes CS as their central element. These CS are limited to the length scales of the boundary layer and are therefore expected to have influence in the proximity of the wall area. Centrifugal forces created by streamline curvature are also known to lead to stationary stream-wise vortices. In convex channels this phenomenon is called the Dean instability and on concave walls the Görtler instability. CS formed in these ways are possible in the slice chambers of curved flow passages [2] or in the upstream area of the slice bars with significant normal direction (ZD) reach. Headbox structures in which an angle is formed between the axis of turbulence generator tubes and the slice chamber naturally lead to secondary flows which may lead to stream-wise CS in some conditions [3]. These structures induced by secondary flows are expected to be of minor importance in headboxes containing vanes separating the rows of turbulence generator tubes [4]. On the other hand, the existence of vanes inherently leads to the formation of CS in the downstream flow. Characteristic to these CS is their slow attenuation. These structures, combined with the reach of the vanes close to the lip area, are believed to produce non-homogeneity in paper. Although the CS are geometrically three dimensional, their MD and CD components are predominant (cf. Kármán vortex street [5]) and have distinctive characters of their own. Especially the CD component of the vortex maintains its

characteristic appearance from the slice chamber to the slice jet. This CD component also has the advantage of being a unique structure compared to the many possible origins of MD vortices described above. As these vortices are produced by modern headboxes, a thorough understanding of them is one of the key components in building a fundamental view of the inheritance of flow structures in paper.

The formation of slice jet topography by the wave instability mechanism has also been studied [6]. Therefore, a careful analysis was carried out in order to show that the CD vortex structure providing the basis of analysis here can be detected both in the slice chamber and on the slice jet. In addition, it can be shown that the changes in the length scale of the vortex structure are supported by theoretical predictions.

This presentation consists of the following three parts. Chapter 2 briefly introduces all the experimental methods used in this research. Chapter 3 discusses the generation of vortices by different types of vanes inside the slice chamber, and the slice jet topography resulting from these vortices. The inheritance of these flow structures in paper is shown by using dye streamers and ink spot analysis. Finally, the scale of coherent vortices is shown to control the scale of cockling. Chapter 4 summarizes all findings.

## **2 EXPERIMENTAL APPROACH**

### **2.1 Introduction**

The main purposes of this study were to clarify the formation of CS in the headbox after the vanes, the influence of CS on slice jet topography, the inheritance of CS in paper, and the effect of CS on the structural cockling of paper. As simultaneous measurement of these phenomena would have introduced formidable challenges, it was decided to study the slice chamber, the slice jet and the paper as separate elements, and then to investigate how the *structural scales* are passed on from one element to another.

As no methods exist to measure flow fields inside opaque suspensions accurately in time and space, the flow analysis in the slice chamber had to be carried out using transparent liquid. The instantaneous CS, characterized by their wavelength and general appearance in the MD-CD and MD-ZD planes, were captured by Digital Particle Image Velocimetry (DPIV). In the slice jet the CS appear in a form of wavy surface topography. This was verified by creating CS of known properties with bluff vanes of 1, 1.5, 2 and 3 mm in thickness and recording the resulting topography by a High Speed Video (HSV) camera. The comparison of corresponding results between DPIV and HSV with water gave equivalent relative changes of wavelengths. Because

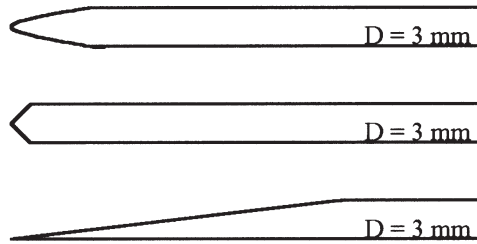


**Figure 1** Realistic vanes: rounded (top), blunt (middle) and sharp (bottom).

experiments with fiber suspension with the same headbox configuration were observed to result in the same wavelength of surface topography, the DPIV analysis with water and the HSV analysis with pulp suspension could be combined to give the linkage between the slice chamber and the slice jet. In addition, bluff vanes of different thickness provide a means of establishing reference information for estimating the effective vane thickness, and the appearance of CS in cases where simple theoretical predictions are not available. CS can also be optically measured in paper with the aid of dye streamers fed into the suspension. Relative changes of wavelength in the slice jet and the average scale of the ink spots of the paper were used to complete the link from flow to paper. Because of the better connection to real papermaking it was useful to create this link by more realistic vanes (Figure 1) than bluff vanes. Finally, using the same paper samples, the structural cockling scales of paper and the CS scales of flow and paper were linked.

The flow experiments in the slice chamber and slice jet were carried out in a separate headbox unit, and specimen paper was collected from a pilot machine trial in which a horizontal gap former was used. The former parameters were adjusted to have minimum effect on the flow structures. The structures were “frozen” quickly by having a jet/wire ratio near one and high initial dewatering. In both the separate headbox unit and the pilot paper machine, a hydraulic headbox with five rows and four vanes was used (Figure 2). For the regular vanes the distance of the vane tips from the slice opening was 100 mm. In experiments on the effect of the number of vanes the top and bottom positions were equipped with 500 mm shorter vanes. This kind of setup was used to avoid flow structures created by the reversed flow areas behind the empty stems. In addition, it was assumed that these short vanes have no part in forming CS. In all experiments the slice opening was held at 14 mm and a fine paper pulp at 0.7% consistency was used as the suspension.

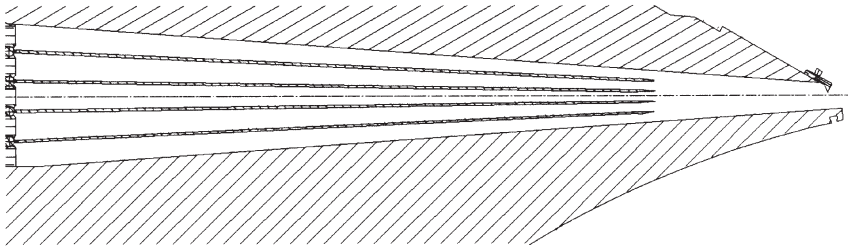


Figure 2 Headbox design.

## 2.2 PIV

Particle Image Velocimetry (PIV) was used for the analysis of the instantaneous 2D velocity fields in a headbox made of plexiglass. DPIV consists of a dual-frame CCD camera, a 2-pulse laser system forming laser sheets and a timing unit to trigger both the camera and the laser. When two images are taken with a specific delay between them, the movement of the seeding particles between these two images describes the velocity of the flow. After the images have been split into smaller segments – so-called interrogation areas of  $32 \times 32$  pixels, for example – the movement of the particles in each interrogation area can be computed with the cross-correlation method and an instantaneous velocity vector field is formed.

Figure 3 shows an instantaneous velocity vector field. A special software package has been built to analyze velocity vector fields, and to compute ‘turbulence quantities’ [7]. One kind of turbulence quantity, called rotation, was calculated by Equation (1) and is shown in Figure 3

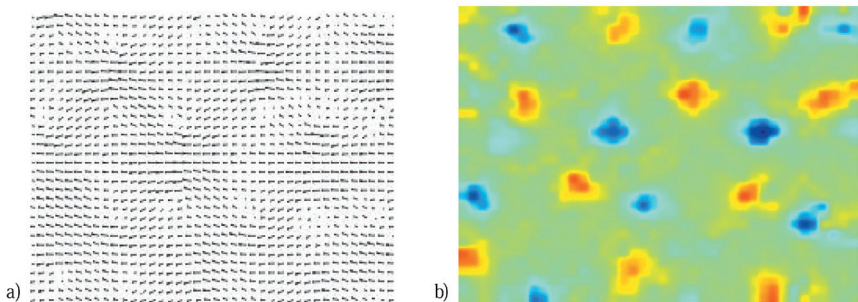


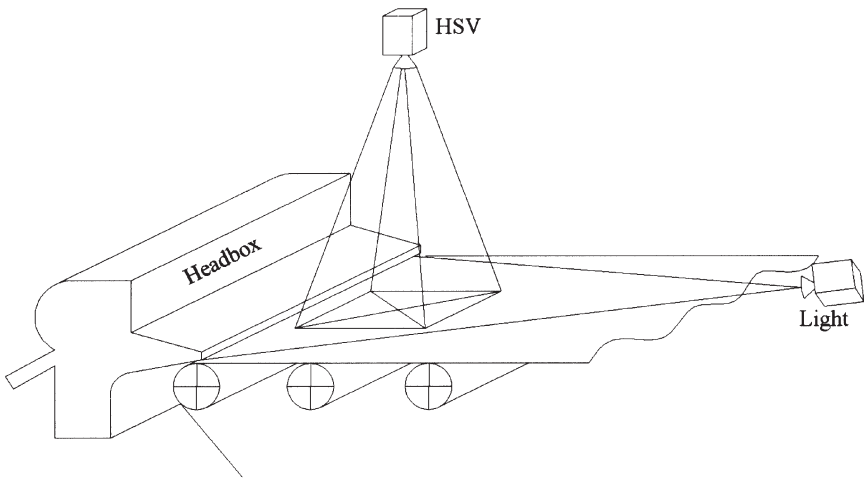
Figure 3 Examples of a) an instantaneous velocity vector field after two vanes and b) a rotation field after four vanes.

$$\omega = \partial u / \partial y - \partial v / \partial x. \quad (1)$$

The CCD camera was located on the side or the top of the headbox just at the end of the two vanes. The size of the imaged area was  $40 \times 32$  mm (CD  $\times$  MD) in the case of side imaging and  $80 \times 64$  mm (CD  $\times$  MD) in the case of top imaging. The calculated rotation fields were further analyzed from 60 images using 2D spectral analysis [8] to find periodic coherent structures in the flow.

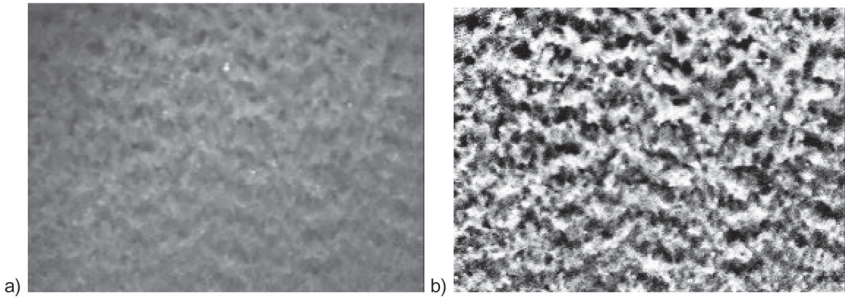
### 2.3 High-speed imaging of the slice jet

A high speed video recording system (HSV) was used to analyze the slice jet surface topography. Illumination with a DC light, incident at a low angle, was utilized to measure the length scales and the periodicities of the surface. A schematic illustration of the imaging arrangement is shown in Figure 4.



**Figure 4** Arrangement for recording slice jet topography.

The periodic structures of the slice jet were analyzed by Fourier spectral analysis (FFT). A sequence consisting of 200 images, in which every image represents an independent sample of  $327 \times 327$  mm in size for each experimental point, was taken with the HSV system. This length of the sequence was found to be large enough in order to produce smooth distributions.



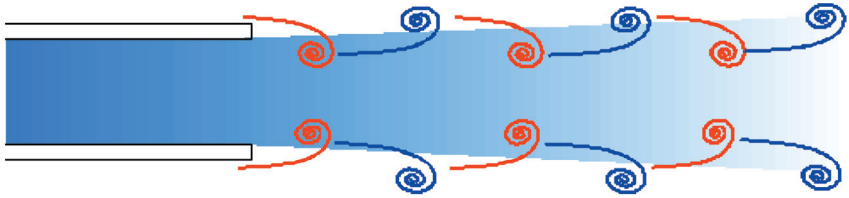
**Figure 5** Surface topography of slice jet; a) original image and b) enhanced image.

Figure 5 shows an example of the original and the illumination-corrected image of the slice jet generated by a headbox with blunt vanes. The illumination field was established by averaging the sequence and, subsequently, filtered to remove topographic structures stagnant in place. This field was then removed from every image of the sequence. The FFT analysis of these enhanced images was used to provide the power density distribution in which the wavelengths of periodic structures are seen as discrete peaks.

## **2.4 Visualization and analysis of CS**

### *2.4.1 Dye streamers*

Black dye was fed into two adjacent primary pipes of a turbulence generator located at the middle of the tube bundle in CD and at the 3rd row of the five rows in ZD. Because of the high turbulence created in the expansion step of the generator, the dye was completely mixed with the base suspension flow and, accordingly, these two dye-marked streams effectively created two adjacent streamers to visualize and mark the vortex streets formed at the trailing edges of the vanes. The Kármán vortex streets are formed by alternating the flow of entering suspension from the different sides of the vane. In this way, the successive vortices have an opposite direction of rotation axis and their core is either filled with dye streamer or with base suspension [5] (Figure 6). This process occurs at the trailing edge of the vanes both below and above the dye-marked row. In addition, it has been experimentally observed that two nearby vortex streets have a strong tendency to stay in opposite phase. This means that vortexes of opposite signs but with the same core content (either dye streamer or base suspension) are found at each MD position (Figure 6). Examples of this kind of vortex behavior are regularly met in the



**Figure 6** Kármán vortex streets of opposite phase for two vanes on top of each other.

layer mixing of stratified headbox systems [9]. As the flow of suspension in the slice chamber is highly turbulent, the part of the dye streamer that is not encompassed by the vortices will be mixed with the base flow. In this way, every second ZD vortex pair will be visible as a spot of dye in the paper web. The distance and size of these spots are related to the frequency of the vortex formation (shedding) and to the amplitude of the vortices, respectively.

#### 2.4.2 Analysis of ink spots in paper

An automated image analysis method was developed for the analysis of ink spots on paper. Paper samples were imaged by an optical scanner in reflect-

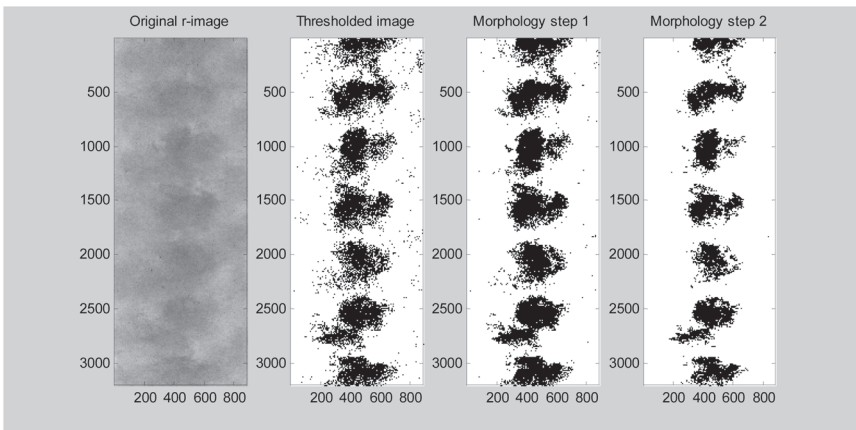


**Figure 7** Image analysis of ink spots. Sub-images from left to right; original r-image, thresholded image, elimination of holes in blobs (morphology step 1) and disconnection of blobs (morphology step 2).

ance mode at a scanning resolution of 300 dpi. The size of the imaged area was 280 mm in the MD direction and 200 mm in the CD direction. An intensity-independent matrix  $r$  ( $r = R/(R + G + B)$ ) was first calculated from the acquired RGB image. Furthermore, color variation due to the uneven distribution of ink in the CD direction was eliminated. In the next step, an empirically determined global threshold was used. In the segmentation 15% of the pixels of the image got value 0 and the rest of the pixels in the image got value 1 (Figure 7). After the segmentation there were many white holes in the spots. Non-linear local operations of binary morphology were used in the elimination of holes in these spots and removal of small spots. The problem with eliminating holes in the spots was that the spots tend to be connected at the same time. In the second step of morphology, a dilation operation was used to eliminate this effect. Finally, a blob-analysis algorithm was used to determine the feret-x and feret-y of the spots and the average area of the spots was calculated by these dimensions (feret-x multiplied by feret-y). In the blob analysis an area criterion for the spots was used because the results were presented as the average area of the spots. The required minimum size for a spot was 900 pixels (in the case of a square blob the required area was 2.5 mm  $\times$  2.5 mm).

## 2.5 Cockling measurement and analysis

An image analysis method was developed for the analysis of deviations from flatness of the paper samples. At first, the paper samples were imaged by a CCD camera and a sidelight was used for the illumination [10]. The CCD camera was mounted perpendicular to the paper surface providing an image

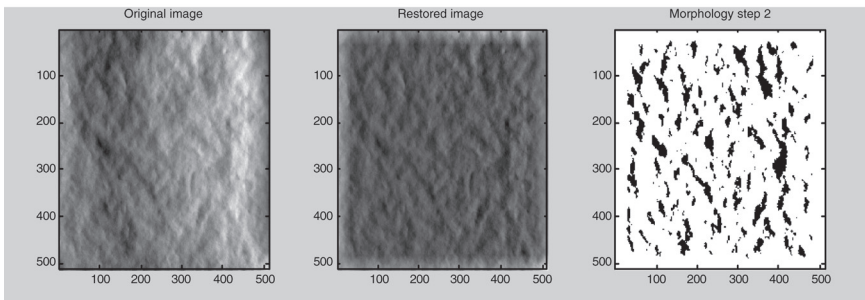


**Figure 8** Image analysis of cockles. Sub-images from left to right; original  $512 \times 512$  image, enhanced image (elimination of uneven illumination distribution), elimination of holes in blobs and disconnection of blobs (morphology step 2).

area of 180 mm × 180 mm. The sidelight produced a clear shadowing on the paper surface. Due to the lighting method the illumination distribution on the paper surface was not uniform. Therefore, the first step in the image analysis method was to eliminate the uneven illumination distribution. A low-pass filtered and scaled image was subtracted from the original image (Figure 8). The new calculated image was then thresholded and post-processed using operations of binary morphology as in the method of analyzing ink spots, described above. In the blob analysis the required minimum size for the cockles was 100 pixels (in the case of a square blob the required area was 3.5 mm × 3.5 mm).

### 3 RESULTS

#### 3.1 Flow studies

Research on CS behind two-dimensional plates has shown that in a Reynolds number range of 100–1,000,000, based on the plate thickness, the MD wavelength is set by geometric properties and is thus independent of the flow velocity. In addition, the wavelength is directly proportional to the plate thickness. These results have regularly been studied in conditions of aerodynamic flow (laminar base flow) or of internal flow with a low Reynolds number based on the channel dimensions [1]. Neither of these conditions correspond to the character of flow inside the slice chamber and the slice jet. However, the results concerning the dependency of wavelengths on the velocity (Figure 9) and the length scale, i.e., the thickness of vane (Figure 10), show that these characteristic properties of CS are found also in paper-making conditions.

The natural vortex shedding frequency of a bluff body at moderate Reynolds numbers can be described by an approximately constant Strouhal number

$$St = \frac{\omega L}{U} = 0.2, \quad (2)$$

in which  $\omega$  is the angular velocity,  $L$  is the plate thickness and  $U$  is the velocity outside the boundary layer. This results in the following estimation for the wavelength  $\lambda$  of vortex shedding in the near-field area of the wake:

$$\lambda = \frac{L}{0.2}. \quad (3)$$

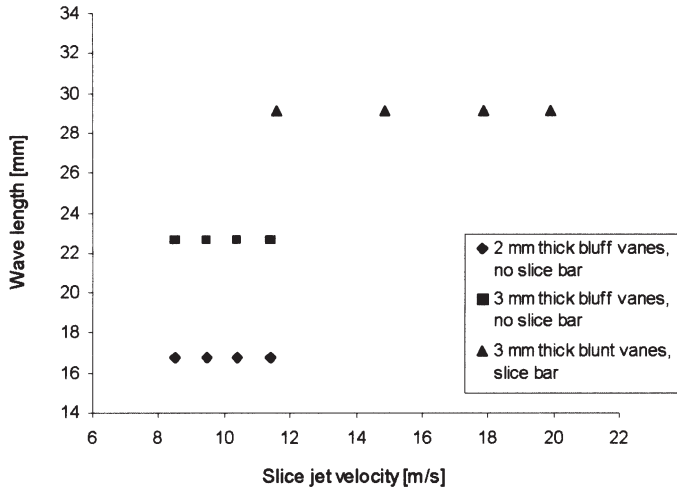


Figure 9 Wavelength vs. slice jet velocity for three different vanes.

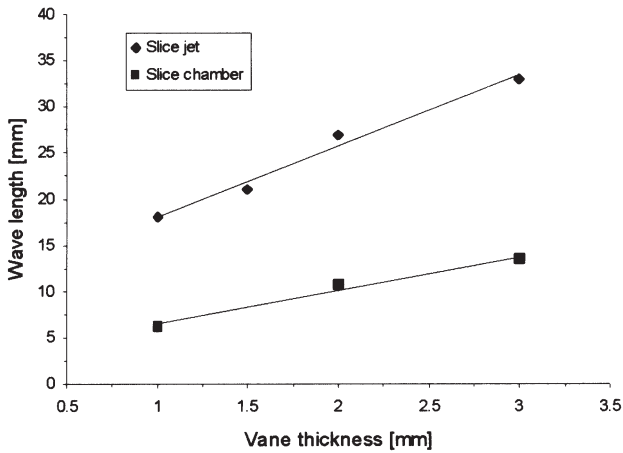
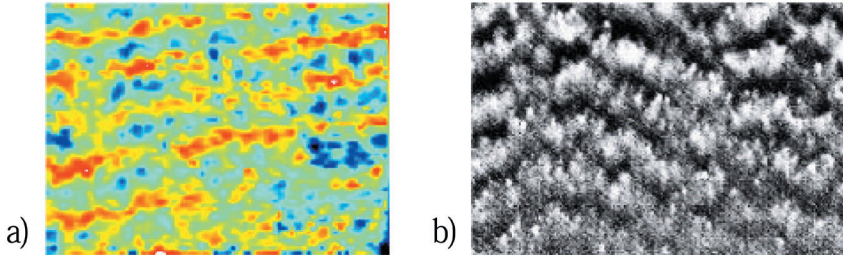


Figure 10 Dependency of wavelength on vane thickness.



**Figure 11** Appearance of coherent structures for 2 mm vanes a) in slice chamber and b) in slice jet viewed in the MD-CD plane.

For a bluff 3 mm thick vane, the equation (3) gives  $\lambda = 15$  mm and the analysis of DPIV data results in  $\lambda = 13.5$  mm (Figure 10). Therefore, the vortex shedding phenomenon of bluff vanes retains its characteristic properties also in the hydrodynamic conditions of the slice chamber. Accordingly, the wavelength of the CS from the bluff vanes can be predicted with a reasonable accuracy and they provide a good reference for more realistic vanes. In the same configuration, the wavelength of the slice jet topography was measured to be  $\lambda = 33$  mm. On the other hand, the geometric ratio of the flow passage height after the vane tip and at the slice jet is approximately 2.5. The stretching-corrected wavelength from DPIV then corresponds to  $\lambda = 34$  mm at the slice jet, which is almost equal to the measured value.

The slice chamber results above were calculated from DPIV images from the headbox side. One interesting question was whether the CS appeared in the slice chamber in the same wave-like form as in the slice jet? To answer this, the flow in the slice chamber was also imaged from the top of the headbox by PIV. Figure 11 shows that the appearance of the CS in the MD-CD plane of the slice chamber has a close resemblance to the CS that are seen in the surface topography of the slice jet. In addition, the information from the DPIV images of the headbox side gives us good reason to assume that the hills of the slice jet topography are strongly related to the ZD linear momentum of flow.

In the slice jet the number of vanes did not affect the position of the wavelength spectrum peak, but the peak became wider with a higher number of vanes (Figure 12). In the case of four vanes, the power at the long wavelengths was clearly increased compared to the case of two vanes. This is probably a consequence of small phase differences between the vortex streets of different vanes arranged on top of each other as illustrated in Figure 6. As expected, the power of the slice jet turbulence, e.g., the area under the power

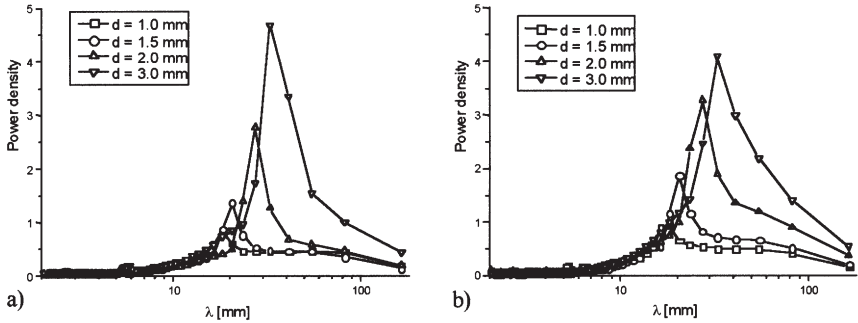


**Figure 12** Power spectrum for a) two and b) four bluff vanes.

spectrum, increased with a larger thickness and higher number of vanes. On the other hand, it seemed that the number of vanes did not affect the height of the spectrum peak and, consequently, the intensity of the CS.

### 3.2 Link between flow and paper

Bluff vanes of different thicknesses provided a means of establishing reference information for estimating the effective thickness of more realistic vanes, which were used to create a link between the flow and the paper. Figure 13 shows the appearance of CS in the slice chamber after sharp, rounded and blunt vanes.

The wavelengths of the CS shown in Figure 13 were 2.7, 7.5 and 14.2 mm, respectively. In reference to the slice chamber results of Figure 10, by using extrapolation at small wavelengths, the effective thickness of realistic vanes were estimated to be 0 mm for the sharp, 1.25 mm for the rounded and 3mm for the blunt vane tip. So, from the viewpoint of the CD component of CS,

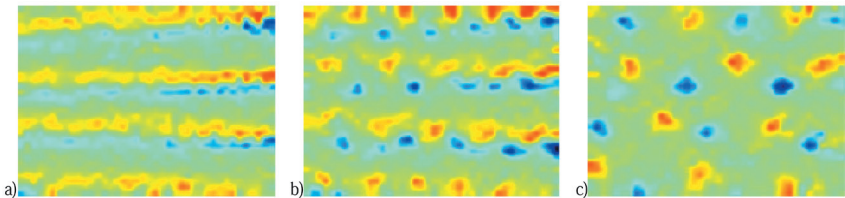


**Figure 13** Appearance of CS after a) sharp, b) rounded and c) blunt vanes.

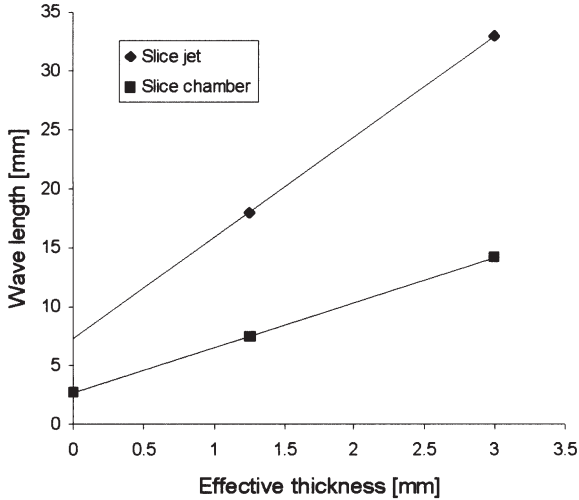


**Figure 14** The wavelength of CS in slice chamber and slice jet for sharp, rounded and blunt vanes.

the sharp vane approached the situation in which no vanes existed and the behavior of the blunt vane was close to the bluff vane. This was also realized in the slice jet, where the CD component for the sharp vanes was too small to be detected by the applied method. The images of the surface topography and the corresponding spectrums of the no vane and the sharp vane setups had a very close resemblance. Likewise for the blunt and the bluff vanes the appearance of the images and the respective wavelengths of the CS were very similar.

The measured wavelengths of the CS in the slice jet for the rounded and the blunt vanes were 18 and 33 mm, respectively. In Figure 14 the wavelengths in the slice chamber and the slice jet are plotted as a function of the effective thickness of vane. The same ratio of wavelengths in the slice chamber and the slice jet is observed as for the case of the bluff vanes.

Dye streamers were used to mark the CS of flow on the paper. It was found that in the case of the four blunt vanes the dye streamers were spread too effectively by the large created CS and their interaction. Therefore, it was decided that to enable the successful analysis of the paper samples produced with this vane type, the bottom and the top vanes were replaced with the short vanes of 100 mm in length. Figure 15 shows the appearance of the CS in paper after the sharp, rounded and blunt vanes.

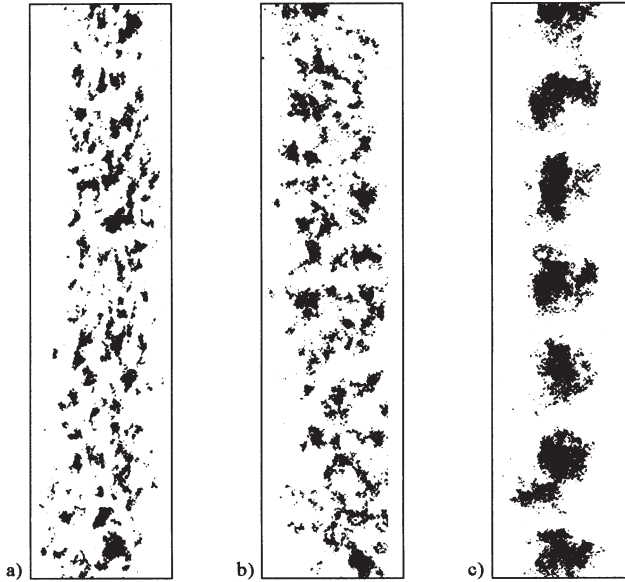


**Figure 15** Appearance of CS in paper after a) sharp, b) rounded and c) blunt vanes.

It is realized that the wave-like form of the CS, observed in the slice jet, has disappeared in all cases except the blunt vanes where the obvious periodicity of the CS has remained. This indicates that the CS of small wavelength and amplitude lose their characteristic appearance faster than the CS of large wavelength and amplitude in the flow before the impingement point. It is also possible that the former destroys effectively the periodicity at short wavelengths but does not much interfere in the periodicity at large wavelengths. However, the average scale of the CS in paper, viewed as the average size of the ink spots, increased with the effective thickness of the vanes, in line with the results for the slice chamber and slice jet. Thus, as illustrated in Figure 16, it can be stated that the scales of the CS in flow were inherited in the paper.

A linear correlation between the scales of the CS of flow and structural cockling of the paper was observed (Figure 17). Accordingly, the CS of small wavelength in the slice chamber led to small-scale structural cockling and the CS of large wavelength led to large-scale structural cockling. While there are many factors on which cockling is dependent [11], the above result shows indisputably that the scale of CS in flow should be considered as one factor of

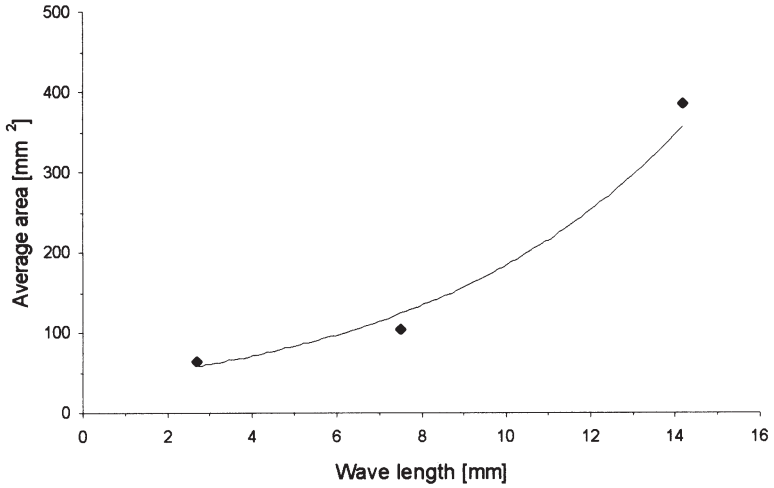


**Figure 16** Average area of ink spots in function of wavelength of CS in slice chamber.

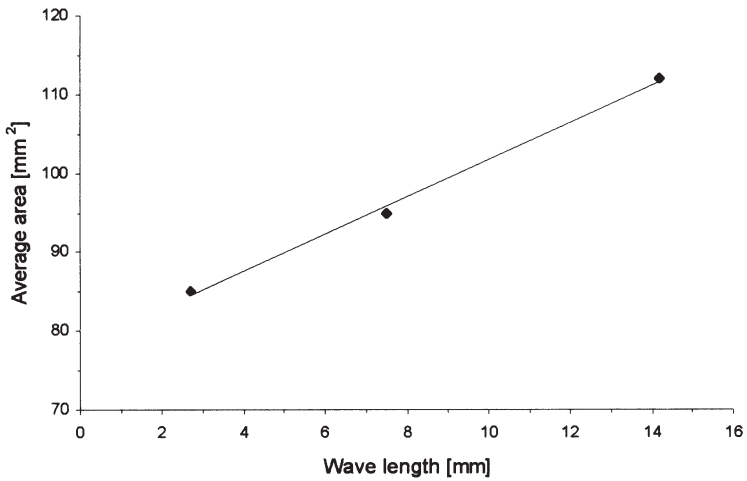


**Figure 17** Average area of paper cockles as function of wavelength of CS in the slice chamber.

high importance. We assume that this is a consequence of the structural unevenness of paper in the scales inherited from the CS of flow.

#### 4 CONCLUSIONS

In this study, a sequence of questions was addressed: What kind of flow structures are generated by vanes inside a hydraulic headbox? How do these flow structures influence the slice jet? Is the structure of the jet inherited by the produced paper? And finally, does this structure have any influence on the characteristics of the paper? To find an experimental answer to all of these questions a multitude of measurement methods were developed and applied for flow analysis of pure liquid, flow of fiber suspensions flow and structure of paper.

The most distinctive flow structures were found to be coherent, time-periodic vortices generated at vane tips inside the slice chamber. In accordance with theoretical results the wavelength of the CD component of these vortices was measured to be a function of vane tip thickness in the case of bluff vanes. The wavelength was found to increase from slice chamber to slice jet according to the ratio of flow velocities at these positions. By a visual comparison, the hypothesis that the origin of the periodic topography of the slice jet was found in the Kármán vortex streets generated by the vanes was further confirmed. An increased number of vanes increased the power spectral densities of long wavelengths. With more realistic vane tips, i.e., sharp, rounded and blunt, similar results were found. The inheritance of the slice jet structure in the paper was analyzed using dye streamers. In the case of blunt vanes, the periodic vortices were transmitted very clearly, as isolated dye spots, into the paper. With thinner vanes the vortices were not strong enough to survive in the forming zone. However, a qualitative relation between wavelength of slice jet and dye spot size was found. Finally, and most importantly, a strong correlation between the wavelength and spatial scale of structural cockling was found.

These new results clearly show that coherent flow structures generated by the headbox have a significant impact on the properties of paper. In this case, the CD components of Kármán vortices, which caused the wavy topography of the slice jet, controlled the scale of localized planar deviations (cockles) of the paper. While not being the only factor controlling cockling, this mechanism seems to explain the origin of the inherent structural non-uniformities leading to the cockling tendency. It can be assumed that three-dimensional fiber orientation is the most important structural property affected by the vortices. This aspect was beyond the present study, but would be important to

address in a future work. The methodology developed in this work can be used to predict a cockling tendency directly from the slice jet without producing paper. On the other hand, in a paper mill environment, paper analyses can be used to evaluate the slice jet and forming conditions.

## REFERENCES

1. Robnsson, S. K., “Coherent motions in the turbulent boundary layer”, *Annual Rev. Fluid Mech.*, **23**: 601–639 (1991).
2. Matsson, O. J. E. and Alfredsson, P. H., “Curvature and rotation-induced instabilities in channel flow”, *J. Fluid Mech.*, **210**: 537–563 (1990).
3. Aidun, C. K., “Hydrodynamics of streaks on the forming table”, *Tappi J.*, **80**(8): 155–162 (1997).
4. Aidun, C. K., “Quantitative evaluation of the forming jet delivered from four different hydraulic headboxes using high speed digital imaging”, *Tappi J.*, **81**(4): 172–179 (1998).
5. Eaton, J. K. and Johnston, J. P., “A review of research on subsonic turbulent flow reattachment”, *AIAA J.*, **19**: 1093–1100 (1981).
6. Söderberg, D., “Hydrodynamics of plane liquid jets aimed at applications in paper manufacturing”, Doctoral thesis. Royal Institute of Technology, Faxén-Laboratoriet, Stockholm (1999).
7. Piirto, M., Eloranta, H. and Saarenrinne, P., “Interactive Software for Turbulence Analysis from PIV Vector Fields”, 10th Int. Symp. on Applications of Laser Techniques to Fluid Mechanics, Lisbon, Portugal (2000).
8. Piirto, M., Eloranta, H., Ihalainen, H., and Saarenrinne P., “2D Spectral and Turbulence Length Scale Estimation with PIV”, Sixth Triennial International Symposium on Fluid Control, Measurement and Visualization, Sherbrooke, Canada (2000).
9. Li, C. A., Rogers, T. D. and Shands, J. A., “Mixing intensity analysis of a 2-layer stratified headbox jet”, *Tappi J.*, **83**(12): 1–16 (2000).
10. Praast, H., Burgdorf, W. and Göttsching, L., “Messtechnische Erfassung und Ursachen von Cockling in Zeitungsdruckpapier. Teil 1. Charakterisierung und Quantifizierung von Cockling”, *Das Papier*, **9**: 147–155 (2000).
11. Niskanen K., Papermaking Science and Technology, Paper Physics, **16**: 255–256 (1998).

## Transcription of Discussion

# COHERENT STRUCTURES OF SUSPENSION FLOW AND THEIR INHERITANCE IN PAPER

*Petri Jetsu*<sup>1</sup>, *Markku Kallomäki*<sup>2</sup>, *Hannu Karema*<sup>2</sup>,  
*Juha Salmela*<sup>2</sup>, *Timo Lappalainen*<sup>2</sup> and *Mika Piirto*<sup>3</sup>

<sup>1</sup>Metso Paper Inc.

<sup>2</sup>VTT Energy

<sup>3</sup>Tampere University of Technology

*Bill Sampson*      Department of Paper Science, UMIST

I noted from your manuscript that you mentioned that you felt that the vanes were very much influencing the orientation of fibres in three dimensions in the sheet, and I wondered if you had seen any changes in sheet density as you change the vanes that would confirm that?

*Petri Jetsu*

Well no we haven't studied that.

*Bill Sampson*

So it is really just speculation at this stage.

*Petri Jetsu*

Well, it is a well known fact that the vanes affect fibre orientation.

*Bill Sampson*

So there is no data to support it.

*Discussion*

*Petri Jetsu*

Not in our study, but in an earlier study yes.

*Iikka Kartovaara*      Stora Enso Oy

You showed measured results only for the scale of the cockles. Can you say anything about the amplitude or intensity of the cockles? Does that vary with the intensity of the turbulence?

*Petri Jetsu*

Well I can't say for sure but I think that if we have very intensive cockling structures and of course the cockle intensity is also very high.